



**HAL**  
open science

## Prediction of organic matter accessibility and complexity in anaerobic digestates

David Fernández-Domínguez, Dominique Patureau, Sabine Houot, Nicolas Sertillanges, Bastien Zennaro, Julie Jimenez

► **To cite this version:**

David Fernández-Domínguez, Dominique Patureau, Sabine Houot, Nicolas Sertillanges, Bastien Zennaro, et al.. Prediction of organic matter accessibility and complexity in anaerobic digestates. Waste Management, 2021, 136, pp.132-142. 10.1016/j.wasman.2021.10.004 . hal-03473235

**HAL Id: hal-03473235**

**<https://hal.inrae.fr/hal-03473235>**

Submitted on 5 Jan 2024

**HAL** is a multi-disciplinary open access archive for the deposit and dissemination of scientific research documents, whether they are published or not. The documents may come from teaching and research institutions in France or abroad, or from public or private research centers.

L'archive ouverte pluridisciplinaire **HAL**, est destinée au dépôt et à la diffusion de documents scientifiques de niveau recherche, publiés ou non, émanant des établissements d'enseignement et de recherche français ou étrangers, des laboratoires publics ou privés.



Distributed under a Creative Commons Attribution - NonCommercial 4.0 International License

# 1 **Prediction of organic matter accessibility and complexity in anaerobic** 2 **digestates**

3

4 David Fernández-Domínguez<sup>a,\*</sup>, Dominique Patureau<sup>a</sup>, Sabine Houot<sup>b</sup>, Nicolas  
5 Sertillanges<sup>a</sup>, Bastien Zennaro<sup>a</sup>, Julie Jimenez<sup>a</sup>

6

7 <sup>a</sup> INRAE, Univ. Montpellier, LBE, 102 Avenue des étangs, 11100, Narbonne, France

8 <sup>b</sup> UMR ECOSYS, AgroParisTech, INRAE, Université Paris-Saclay, 78850, Thiverval-  
9 Grignon, France

10

11 \* Corresponding author: david.fernandez-dominguez@inrae.fr

12

## 13 **Abstract**

14 Further characterization to properly assess the fate of organic matter quality during  
15 anaerobic digestion and organic carbon mineralization in soils is required. Organic  
16 matter quality based on its accessibility and complexity was employed to successfully  
17 classify 28 substrate/digestate pairs through principal components and hierarchical  
18 clustering analysis. The two first components explained 58.02% of the variability and  
19 four main groups were separated according to the feedstock type. A decrease in the  
20 accessibility (16-66%) and an increase in the complexity (34-98%) of the most  
21 accessible fractions was noticed. Besides, an increase of non-biodegradable compounds  
22 (17-66%) was globally observed after anaerobic digestion. The observed trends in the  
23 conversion of organic matter during anaerobic digestion have allowed to fill the gap in  
24 the modeling of the anaerobic digestion process chain. Indeed, partial least squares  
25 regressions have accurately predicted the organic matter quality of digestates from their  
26 inputs ( $R^2 = 0.831$ ,  $Q^2 = 0.593$ ) although the digester operational conditions

27 (temperature and hydraulic retention time) were non-explicative enough. As a novel  
28 approach, the predicted digestate quality was used to feed a partial least squares  
29 regression model previously developed to predict organic carbon mineralization in soil.  
30 The combined models have predicted experimental organic carbon mineralization in soil  
31 ( $R^2 = 0.697$ ) with a model quality similar to the model for organic carbon mineralization  
32 in soil ( $R^2 = 0.894$ ). This is the first study that has successfully conceived an additional  
33 step in the prediction of organic matter fate from raw substrate before anaerobic  
34 digestion to soil carbon mineralization.

35

## 36 **Abbreviations**

37 3D, three dimension; AD, anaerobic digestion; BMP, biochemical methane potential; C, carbon; C<sub>bio</sub>,  
38 biodegradable carbon; COD, chemical oxygen demand; DOM, Dissolved Organic Matter; EPS,  
39 extracellular polymeric substances; FCI, fluorescence complexity index; HRT, Hydraulic Retention Time;  
40 HCA, Hierarchical Clustering Analysis; NEOM, Non-Extractable Organic Matter; NMR, nuclear  
41 magnetic resonance; OM, organic matter; PCA, Principal Components Analysis; PEOM, Poorly  
42 Extractable Organic Matter; PLS, Partial least squares;  $Q^2$ , Percent of variation of Y predicted by model  
43 in cross-validation,  $R^2$ , Correlation coefficient from PLS; REOM, Readily Extractable Organic Matter;  
44 RMSE, Root Mean Square Error, RMSE<sub>CV</sub>, Root Mean Square Error for Cross Validation; RMSEP,  
45 RMSE calculated on validation dataset; PC1, Principal Component 1; PC2, Principal Component 2; Pf(i),  
46 fluorescence proportion for a zone (i); SEOM, Slowly Extractable Organic Matter; SPOM, Extractable  
47 Soluble from Particulate Organic Matter; T, Temperature; TS, total solids; Vf (i), fluorescence volume for  
48 a zone (i); VS, volatile solids

49

50

## 51 **Keywords**

52 biogas effluent, stability, fluorescence, waste characterization, soil

53

## 54 **1. Introduction**

55 The current waste management model has started to evolve towards more sustainable  
56 and resource recovery strategies (Fonoll et al., 2016; Vidal-Antich et al., 2021).

57 Anaerobic Digestion (AD) is a biological process widely used to convert the organic

58 matter (OM) present in different wastes into methane (Fernández-Domínguez et al.,  
59 2020; Vinardell et al., 2021), along with the production of both OM and nutrient-rich  
60 by-product called digestate (Fernandez-Bayo et al., 2018; Guo et al., 2018). Nowadays,  
61 digestates represent alternative fertilizers used in agriculture either as organic  
62 amendment or fertilizer depending on the process, post-treatment and substrate type  
63 (Akhiar et al., 2017; Guilayn et al., 2020). However, digestate efficiency as organic  
64 amendment mainly depends on their OM stability (Kögel-Knabner, 2002), which  
65 remains a topic of ongoing research.

66 A need for accurate OM characterization added to the strict limitations by legislation on  
67 contaminants, such as heavy metals for the agricultural reuse of specific feedstock, are  
68 points of main consideration to enhance digestate management (Khakbaz et al., 2020).  
69 Digestate stability has to be properly assessed before land application (Tambone et al.,  
70 2013; Maynaud et al., 2017). Digestates often acquire higher biological stability and  
71 nutrient availability (particularly nitrogen) than raw substrates, enhancing the interest  
72 for land use (Provenzano et al., 2011). During AD, recalcitrant compounds are  
73 concentrated since the labile organic structures are preferentially degraded (Insam et al.,  
74 2015). Nonetheless, this stabilization could occur due to the interaction of different  
75 factors, including (i) degradation and solubilization of simple compounds, (ii) molecular  
76 complexification, (iii) complex microbial-related products release from biomass growth  
77 and decay (Aemig et al., 2016).

78 For a suitable agronomic valorization of digestates, evaluating the OM fate during AD  
79 and soil carbon (C) mineralization is a meaningful aspect to reduce associated  
80 environmental impacts (e.g. C loss, greenhouse gases emission) or favor ecosystem  
81 service like soil C sequestration that contributes to climate change mitigation (Minasny  
82 et al., 2017). Thus, wider efforts are needed to better understand how OM from non-

83 digested substrate is transformed into digestate OM (Shakeri Yekta et al., 2019;  
84 Tambone et al., 2015).

85 Standard methods to measure the biodegradability of organic wastes through  
86 biodegradability assays are laborious and time-consuming. At least, 30 and 90 days are  
87 required for anaerobic biodegradation potential tests and aerobic biodegradation during  
88 soil incubations, respectively (Jimenez et al., 2017). Hence, biochemical fractionation is  
89 a much more time-saving method to characterize the structural nature of organic wastes  
90 and assess waste biodegradability using successive chemical extractions (Teglia et al.,  
91 2011a). The Soest (1963) fractionation method was widely applied to associate OM  
92 composition with biodegradability (Fernandes et al., 2009; Gunaseelan, 2007; Triolo et  
93 al., 2012). Based on this fractionation method, the Iroc indicator (i.e. indicator of  
94 residual organic C in soils) has been developed as a proxy of the potentially remaining  
95 OM after application in soils for various organic amendments (Lashermes et al., 2009).  
96 Moreover, it was successfully used to predict the long term evolution of OM in soils  
97 after repeated applications of these organic amendments (Levavasseur et al., 2021).  
98 However, biodegradable substrates and digestates were not included in the panel of OM  
99 used for the development of the Iroc indicator. In addition, the Soest fractionation  
100 method presented limitations in predicting the biodegradability for a wide range of  
101 organic residues using biomethane potential tests (BMP) (Mottet et al., 2010).  
102 Therefore, less aggressive methods were requested as a more representative way for  
103 anaerobic biodegradability prediction (Bareha et al., 2018; Mottet et al., 2013).

104 With this purpose, Jimenez et al. (2015) suggested a less aggressive fractionation  
105 method coupled with 3D fluorescence on the extracted fractions. These authors  
106 successfully classified sixty organic residues based on their OM quality, which is  
107 defined by the OM accessibility (i.e. compounds availability to microorganisms for intra

108 or extra-cellular degradation) and complexity (i.e. molecules structure) of organic  
109 waste. This methodology is a promising approach compared with single spectroscopic  
110 techniques. Indeed, it has allowed an accurate assessment of the OM quality (Muller et  
111 al., 2014; Zhang et al., 2019) and has defined new inputs for AD modeling approaches  
112 (Jimenez et al., 2020). Interestingly, in Jimenez et al. (2017), the OM quality of 82  
113 samples, comprising organic waste of different origin, was used to accurately predict  
114 both BMP and potential C mineralization in soil using Partial Least Square (PLS)  
115 regression. Similarly, Bareha et al. (2018) have properly evaluated the correlation  
116 between substrates organic nitrogen accessibility indicators with C biodegradability  
117 using an extracellular polymeric substances (EPS) fractionation method modified from  
118 Jimenez et al. (2015) in PLS regressions. The accessibility and complexity of a treated  
119 substrate will probably vary during AD. However, no studies have been focused before  
120 on the prediction of digestate OM quality from their corresponding inputs. This  
121 approach would make it possible to further predict the potential C mineralization of  
122 digestates in soil as described in Jimenez et al. (2017). Therefore, models could be an  
123 interesting alternative to fill this gap, saving time and providing new tools to improve  
124 AD performance.

125 Feedstock typology stands as a key factor to understand the final OM quality of  
126 digestates (Rocamora et al., 2020). Indeed, Fourier-transform infrared spectroscopy  
127 (FTIR) analysis showed that the main spectroscopic features in digestates depend on the  
128 composition of the initial biomass (Provenzano et al., 2011). Nevertheless, structural  
129 changes of labile and recalcitrant fractions of OM were reported comparing the nuclear  
130 magnetic resonance (NMR) spectra of different substrates and their subsequent  
131 digestates (Laera et al., 2019; Shakeri Yekta et al., 2019). However, the OM quality  
132 evolution due to AD has not been evaluated for a broad range of feedstock. Nonetheless,

133 it could provide relevant information for different sectors implementing AD (e.g. farms,  
134 wastewater treatment plants, solid waste treatment plants).

135 This study aims to assess the OM accessibility and complexity evolution during AD for  
136 a wide variety of feedstocks. To this end, 28 substrate/digestate pairs including different  
137 feedstock nature were classified using statistical analyses to evaluate how both  
138 feedstock type and AD parameters influenced OM quality in the final digestate. Finally,  
139 a model based on linear regression was proposed to predict digestate OM quality from  
140 their inputs. The predicted quality was used to feed the PLS model for C  
141 biodegradability in soil proposed by Jimenez et al. (2017) to determine the digestates  
142 organic C mineralization in soil after land spreading.

143

## 144 **2. Material and methods**

### 145 **2.1. Substrate/digestate pairs**

146 Twenty-eight substrate/digestate pairs (a total of 56 samples) were collected from  
147 different waste treatment plants in France. The selected organic substrates, including  
148 diverse types of feedstocks and origins, were anaerobically digested in laboratory or  
149 full-scale reactors under different digester operational conditions (Table 1). The studied  
150 samples comprised 6 digestate types from the digestate fertilizing-value typology  
151 reported in Guilayn et al. (2019). Each sample was characterized in terms of  
152 accessibility and complexity as assessed by the biochemical fractionation method  
153 coupled with 3D fluorescence developed in Jimenez et al. (2015) and described below.  
154 Biochemical fractionation was conducted on the freeze-dried particular matter and  
155 fluorescence on the aqueous phase.

## 156 **2.2. Fractionation method**

157 Following the reported methodology in Jimenez et al. (2017), all the fresh samples were  
158 centrifuged (ca. 18,600 g for 30 min) at 4°C as a first step. The aqueous phase, namely  
159 dissolved organic matter (DOM), was separated. Total Solids (TS) and Volatile Solids  
160 (VS) on the raw sample as in the resulting particulate phase were determined (APHA,  
161 2005). Then, the particulate phase was freeze-dried and ground (1 mm) and a quantity  
162 of 0.5 g of freeze-dried sample was subjected to the successive chemical extractions (30  
163 mL of each extractant). After every extraction stage, the sample was centrifuged  
164 (18,600 g, 20 min, 4 °C) and the liquid phase was filtered (0.45 µm) and kept for  
165 analyses. All tests were carried out in duplicate. The resulting fractions from the  
166 fractionation method, ordered from more to less accessible, were defined as: (1)  
167 Extractable Soluble from Particulate Organic Matter (SPOM), (2) Readily Extractable  
168 Organic Matter (REOM), (3) Slowly Extractable Organic Matter (SEOM), (4) Poorly  
169 Extractable Organic Matter (PEOM), (5) Non-Extractable Organic Matter (NEOM).  
170 Chemical oxygen demand (COD) and 3D fluorescence spectroscopy were performed on  
171 the four liquid extracted fractions (DOM, SPOM, REOM, PEOM). Regarding the  
172 fractionation method reproducibility, the measurement error is below 5% (data not  
173 shown).

174 COD was determined on the extracts in duplicate using Aqualytic® Vario COD kits (0-  
175 1500 mg O<sub>2</sub>/L) analyzed using an ultraviolet (UV) spectrophotometer MultiDirect from  
176 Aqualytic®. Samples were diluted with deionized water if required. Units were in  
177 mgO<sub>2</sub>/L and mg O<sub>2</sub>/g TS for the liquid and solid phases, respectively.

## 178 **2.3. Fluorescence spectroscopy analysis**

179 The 3D fluorescence spectroscopy analyses were conducted on the obtained liquid  
180 fractions using a spectrofluorimeter Perkin Elmer LS55. The excitation wavelengths



181 varied from 200 to 600 nm and the values were recorded every 0.5 nm between 200 and  
 182 600 nm, with increments of 10 nm. The resulting spectra were divided into seven  
 183 different zones (I-VII) corresponding to a biochemical family with common complexity  
 184 level for spectra interpretation, as described by Jimenez et al. (2014) and He et al.  
 185 (2011): I, protein-like (Tyrosine); II, protein-like (Tryptophane), III, protein-like  
 186 (Tyrosine, Tryptophane and microbial products); IV, fulvic acid-like; V, inner filter,  
 187 glycolated protein-like; VI, melanoidin-like and lignocellulose-like; VII, humic acid-  
 188 like. Afterward, the obtained data were processed to calculate the fluorescence volume  
 189 of each zone  $V_f(i)$  and then the fluorescence proportion of each zone  $P_f(i)$  as described  
 190 in Eqs. (1) and (2), respectively.

$$191 \quad V_f(i)(U.A./mg \text{ COD} \cdot L^{-1}) = V_{f\_raw}(i)/COD_{sample} \times 1/\frac{S(i)}{\sum_{i=1}^7 S(i)} \quad (\text{Eq.1})$$

$$192 \quad P_f(i)(\%) = V_f(i)/\sum_{i=1}^7 V_f(i) \times 100 \quad (\text{Eq.2})$$

193

194 Where:

195  $V_f(i)$  is the normalized volume of a zone  $i$  (U.A./ mg  $O_2 \cdot L^{-1}$ )

196  $V_{f\_raw}$  is the raw fluorescence volume of a zone  $i$  (U.A./ mg  $O_2 \cdot L^{-1}$ )

197  $COD_{sample}$  is the COD concentration of the sample (mg  $O_2 \cdot L^{-1}$ )

198  $S(i)$  is the area of a zone  $i$  (nm<sup>2</sup>)

199  $P_f(i)$  is the fluorescence proportion of a zone  $i$  (%)

200 Moreover, a fluorescence complexity index (FCI) was calculated between the  
 201 proportions of fluorescence volumes of the most complex molecules zones (IV-VII) and  
 202 the less complex molecules zones (I-III), as stated in Eq. (3) (Aemig et al., 2016).

$$203 \quad FCI = \frac{\sum_{i=4}^7 V_f(i)}{\sum_{j=1}^3 V_f(i)} \quad (\text{Eq.3})$$

204

## 205 **2.4. Statistical analysis**

206 Principal component analysis (PCA), Hierarchical Clustering Analysis (HCA) and their  
207 corresponding plots were carried out in R (4.0.3) (R Development Core Team, 2021).  
208 The displayed groups for the PCA individuals were determined by HCA clustering.  
209 Both analyses were conducted on a total of 56 samples (28 substrate/digestate pairs)  
210 considered individually. A Euclidean distance matrix with center-scaled variables was  
211 calculated before HCA analysis and the number of groups was determined heuristically.  
212 PCA was performed on center-scaled variables. A total of 34 variables for each sample  
213 was evaluated. Six variables were related to the accessibility of the sample and  
214 corresponded to the biochemical fractions (DOM, SPOM, REOM, SEOM, PEOM,  
215 NEOM) and 28 variables were linked to the complexity of the sample (seven  
216 fluorescence variables for each extracted fraction). Tukey's methodology was followed  
217 for the displayed boxplots.

218 In order to determine a linear prediction model of digestate quality from substrates  
219 quality, PLS regressions were performed using SIMCA software from UMETRICS. In  
220 its simplest form, a linear model specifies the linear relationship between a dependent  
221 (response) variable Y, and a set of X predictor variables, the X's. Cross-validation was  
222 then performed to test the model's quality. K-fold cross-validation was used. The  
223 database was divided into 7 blocks and some samples were selected as validation  
224 samples. This step was repeated. The mean and standard deviation of the scores were  
225 calculated to estimate the bias and the variance of validation performance. The  
226 validation step was performed on 5 samples not used in the calibration step among the  
227 28 samples, chosen as representative of each type of digestate: Sludge\_2\_D, PS + Cow  
228 Food\_D, PS + Cow Manure\_D, MW4\_D and CM3\_D.

229 The parameters from the PLS models used to assess model quality are the following:

230 Correlation coefficient:  $R^2$ .  
231 Root Mean Square Error (RMSE): used as an accuracy measurement of differences  
232 between predicted values and measured model values.  
233 RMSE\_CV: which is the RMSE for the cross-validation and was applied as prediction  
234 model error.  
235 RMSEP: RMSE calculated on the validation dataset.  
236  $Q^2$ : percentage of variation of Y predicted by the PLS model according to cross-  
237 validation. This parameter indicates how well the model predicts the data. A large  $Q^2$   
238 ( $>0.5$ ) indicates good predictivity.  
239 The PLS model was based on 33 variables: the fractionation percentage of COD  
240 (DOM+SPOM, REOM, SEOM, PEOM, NEOM) and the fluorescence percentage of the  
241 seven zones coming from each fraction. The PLS model coefficients are presented in  
242 Supplementary Material. The same X-Variables as Jimenez et al. (2017) model have  
243 been used. Thus, DOM and SPOM fractions have been pooled and only SPOM  
244 fluorescence percentage has been considered. To combine the PLS model for C  
245 biodegradability in soil from Jimenez et al. (2017) and the digestate quality PLS model,  
246 experimental data obtained from soil C mineralization tests as described in Jimenez et  
247 al. (2017) have been used. Fourteen digestates have been tested among the 28 samples  
248 previously defined. Table 2 presents the digestates considered and their respective  
249 biodegradable C percentage.

250

## 251 **3. Results and Discussion**

### 252 **3.1. Substrates and digestates classification**

253 PCA and HCA analyses were conducted on 33 variables describing the accessibility and  
254 complexity of the OM for the 56 samples considered individually. Scores and loadings  
255 from PCA are presented in Figure 1a and 1b, respectively. HCA clusters are illustrated  
256 in Figure 1c. The PCA analysis has showed that the first two components explained  
257 58.02% of the total variance, meaning that the samples were rather well described by  
258 the used characterization data. These results are in accord with previous studies  
259 focusing on organic waste classification (Jimenez et al., 2015) or the characterization of  
260 post-treated digestates (Maynaud et al., 2017). From the HCA, four main groups were  
261 identified by different colors (A, B, C, D) in PCA and HCA plots (Figure 1a and 1c).

262 The Component 1 (PC1) was described by the complexity of the molecules, from the  
263 simplest samples on the right part of the loadings plot (mainly fluorescences zones II-  
264 III, related to simple sugars/proteins and microbial products with low complexity) to the  
265 most complex samples on the left part (mainly fluorescences zones VI-VII, linked to  
266 humic acids, lignocellulose and melanoidin). Hence, PC1 was significantly (p-value <  
267 0.05) correlated to simple and intermediate fluorescence zones, such as REOM\_I\_II,  
268 SEOM\_I\_II and PEOM\_I\_IV variables ( $R^2 = 0.77, 0.67$  and  $0.66$ , respectively).

269 Meanwhile, it was anti-correlated (p-value < 0.05) to complex fluorescence zones (VI-  
270 VII), particularly REOM\_I\_VII, REOM\_I\_VI and SEOM\_I\_VI variables ( $R^2 = -0.94, -$   
271  $0.90$  and  $-0.87$ , respectively).

272 The second component (PC2) was explained by the complexity added to the  
273 accessibility of the sample. A significant (p-value < 0.05) and positive correlation was  
274 observed between REOM\_C ( $R^2 = 0.74$ ) and fluorescence zones from I to III  
275 (SPOM\_I\_III, REOM\_I\_I and SEOM\_I\_I, with  $R^2 = 0.78, 0.67$  and  $0.65$ , respectively).

276 Contrarily, a significant (p-value < 0.05) and negative correlation was defined between  
277 PEOM\_C ( $R^2 = -0.79$ ) and fluorescence zones of intermediate complexity as

278 REOM\_I\_IV, SEOM\_I\_IV, SEOM\_I\_V ( $R^2 = -0.95, -0.85, \text{ and } -0.85$ , respectively).

279 Biochemical fractionation variables were among the main variance contributors for PC2

280 which allowed to identify the most accessible samples on the top (essentially due to

281 REOM) from the less accessible samples (mainly PEOM) on the bottom. DOM fraction

282 was not correlated with SPOM/REOM/SEOM nor to PC1 but to a lesser extent ( $R^2 = -$

283  $0.59$  and  $p\text{-value} < 0.05$ ). SEOM was positively correlated with the most accessible

284 fractions (SPOM and REOM) while PEOM was negatively correlated with REOM and

285 SEOM, as previously stated by Jimenez et al. (2015) and Aemig et al. (2016). Zhang et

286 al. (2019) also showed that SEOM fraction shared protein-like compounds fluorescent

287 peaks with SPOM and REOM fractions whereas PEOM presented a humic-like

288 compound peak as the main peak. Indeed, NMR spectroscopy on the solid fraction

289 showed that SEOM was mainly composed of proteins (Laera et al., 2019). NEOM

290 fraction was non-explicative enough in this study.

291 Figure 1c shows the four groups established from the HCA analysis based on the

292 extracted fractions and their complexity of each sample: (A) pig slurry and slurry

293 mixtures with primary sludge, agro-industrial waste or biowaste, (B) manure, fibers and

294 municipal solid waste, (C) pig slurry mixtures with fiber or food wastes, and (D) sludge.

295 All the groups were strictly related to the feedstock type, highlighting its influence on

296 organic waste classification, which is supported by other authors (Akhiar et al., 2021;

297 Bareha et al., 2018; Guilayn et al., 2019). Groups B, C, and D came from a different

298 main cluster than Group A, probably due to a higher DOM content related to complex

299 fluorescence zones (VI-VII) that could arise from the degradation of refractory

300 compounds of other fractions (Zhang et al., 2019). The high reported complexity in

301 animal slurries could be related to particular recalcitrant alkyl-C (e.g. sterols, lipids,

302 cutin) (Tambone et al., 2019). Group B was defined by PEOM (poorly accessible C)

303 and fluorescence zones IV and V. Indeed, these types of substrates are characterized to  
304 present high C/N and TS besides complex proteins and humic/fulvic acids (Akhiar et  
305 al., 2017). Finally, Groups C and D were related to low complexity zones (I-III) while  
306 sludge showed higher fluorescence proportions on zones III than pig slurry mixtures. In  
307 fact, zone III corresponds to protein content and microbial by-products, typically related  
308 to activated sludge metabolism and growth/decay (Fang et al., 2015). These results have  
309 been also reported by Zhang et al. (2019), who showed that the characteristic presence  
310 of protein-like organics (zones II and III) was in the SPOM and REOM fractions of  
311 sludge.

312 Interestingly, a broad variance on pig slurry mixtures clustering from fluorescence  
313 zones I-III to VI-VII was found depending on the co-substrate added (e.g. pairs of pig  
314 slurry + fiber co-substrate were clustered in Group C but spatially distributed close to  
315 Group B, which is mainly composed of fiber-rich samples). Notwithstanding that the  
316 percentage of co-substrate in raw mass was mainly below 20%, the addition of a co-  
317 substrate seems to influence their classification and should be considered to properly  
318 classify organic wastes (see Table 1).

319 Most of the digestates were clustered together with their substrates, confirming that the  
320 main OM complexity and accessibility prevailed after AD (Provenzano et al., 2014).  
321 Nevertheless, within the same cluster, variations in the classification between substrates  
322 and digestates have been observed. Since the OM accessibility and complexity  
323 conversion after AD remains unclear, it is discussed in the following section.

## 324 **3.2. OM accessibility and complexity: revealed groups characterization**

### 325 ***3.2.1. OM accessibility and fluorescence complexity index of substrates***

326 The proportion of total COD in the biochemical fractions and the FCI (defined in  
327 Section 2.3) of substrates profiles have been evaluated to define each group and are  
328 summarised in Figure 2.

329 The proportions of COD for each extracted fraction varied between groups according to  
330 the different origins of the sample (Figure 2). The largest proportion of COD for Group  
331 A was in the DOM fraction (30-55%), indicating a notable content of water-soluble  
332 organic substances in slurries, such as simple sugars (e.g. sucrose, glucose and  
333 fructose), proteins (mainly globular protein), volatile fatty acids or soluble recalcitrant  
334 compounds. High DOM fraction content was also reported by Laera et al. (2019) (76%  
335 of total COD) for a substrate from a household, slaughterhouse and industrial waste co-  
336 digestion plant. For Groups B and C, PEOM fraction was the main COD fraction  
337 extracted and ranged between 22 and 58% of total COD. Indeed, these results are  
338 consistent since the PEOM fraction is rich in hemicellulose, cellulose-like, starch and  
339 certain proteins (Laera et al., 2019), which characterizes the fibrous feedstocks of  
340 Groups B and C. Finally, Group D extracted COD was dominated by the NEOM  
341 fraction (23-33%). Similar values of NEOM (30-40%) have been reported by different  
342 authors for sludge samples (Jimenez et al., 2015; Maynaud et al., 2017).

343 Comparing the accessibility between groups, Group D had the highest SEOM (27%)  
344 and SPOM (22%) fractions probably due to high complex protein content (mainly  
345 fibrous proteins) and simple sugars/proteins in sludge samples. Group C presented the  
346 highest REOM (25%) and NEOM (39%) fractions probably because of the protein and  
347 lipid content provided by food wastes. Group B presented the highest PEOM fraction  
348 (58%), while the NEOM fraction was the second extracted fraction for all the groups  
349 (except for Group D), indicating that all wastes had a considerable amount of non-

350 extractable OM. Whilst, SPOM and REOM fractions showed low percentages of the  
351 total extracted COD for all the groups.

352 Regarding the FCI of the substrates, Groups A and B had higher FCI in all fractions  
353 compared with Groups C and D (Figure 2). Indeed, Group C and D were mainly  
354 characterized by fluorescence regions I to III likely they have less complex  
355 proteins/lignified compounds than Groups A and B. Only the FCI of the SPOM fraction  
356 of Group C (1.03-1.50) was higher than the one of the other Groups. The highest FCI  
357 for all groups was for Groups A and B and corresponded to the less accessible fractions  
358 (SEOM and PEOM), as reported by Muller et al. (2014). Concerning the FCI of each  
359 group, the FCI of the SEOM fraction was the highest for the Group A (3.60). In fact,  
360 this fraction targets recalcitrant compounds such as humic-like acids, fulvic-like acids  
361 and complex proteins, which could explain that Group A was previously defined by  
362 complex fluorescence zones (VI-VII) (see Figure 1). The FCI of the PEOM fraction  
363 showed the highest values for Group B and D (2.94 and 1.97, respectively) whereas  
364 Group C displayed slight differences in the FCI for all the extracted fractions.

365 Fluorescence spectroscopy was also performed on some DOM fractions samples (PS,  
366 CM/S and HM/S + Slu, BW + CS + AI, Sludge\_6 and Sludge\_7). However, this data  
367 was not considered in this study because (i) all the DOM fractions in the dataset were  
368 not analyzed and (ii) Jimenez et al. (2017) did not consider it in their model.

369 Nonetheless, the fluorescence percentage for zone I to VII of SPOM and DOM of these  
370 6 samples were similar for the evaluated substrates. Zhang et al. (2019) reported similar  
371 results for sewage sludge. Therefore, DOM fluorescence was not relevant for an  
372 accurate prediction of the final C mineralization in soil concerning the present study  
373 (see Supplementary Material).



### 374 **3.2.2. OM accessibility and fluorescence complexity index conversion after AD**

375 The anaerobic biodegradability of OM also depends on the chemical nature of the  
376 compounds, therefore, the more accessible fractions will not strictly be the more  
377 biodegradable fractions (Bareha et al., 2019; Mottet et al., 2010). However, simpler  
378 compounds (e.g. soluble sugars or proteins) will be extracted in the most easily  
379 extractable fractions, while lignocellulose-like compounds are normally present in the  
380 last extracted fractions. To evaluate these considerations, Table 3 shows the proportions  
381 of COD for each extracted fraction and the FCI evolution between the substrates and  
382 their corresponding digestates after AD. Meanwhile, Figure 3 displays the proportions  
383 of COD for each extracted fraction (described in Section 2.2) and FCI profiles for the  
384 digestates samples of each group.

385 From the four groups evaluated, general assumptions can be drawn regarding the  
386 influence of AD in the OM quality of digestates. The SPOM and REOM fractions have  
387 decreased after AD whereas the FCI increased for all feedstock groups (except SPOM  
388 and REOM complexity of Group C which decreased). Aemig et al. (2019) have also  
389 reported the highest biodegradation yields for the most accessible fractions (74% and  
390 69% for SPOM and REOM, respectively) after sewage sludge AD. Thus, SPOM and  
391 REOM have shown the lowest percentage of extracted COD (less than 10% of total  
392 COD) for all digestates. Indeed, the sum of SPOM+REOM in digestates ranged between  
393 3 and 27% of the total COD samples (data not shown). Low extracted COD proportions  
394 for the most accessible fractions were also found in Bareha et al. (2018) and Laera et al.  
395 (2019), where the sum of SPOM, REOM and SEOM was below the 10% of total COD.  
396 Similarly, the sum of SPOM + REOM only accounted for the 2.7-10.6% of the total  
397 COD of digestates OM by Maynaud et al. (2017). In accordance with the present study,  
398 Aemig et al. (2019) and Zhang et al. (2019) have also reported an increase of the FCI

399 for SPOM and REOM fractions since simple fluorescence peaks remarkably decreased  
400 after anaerobic digestion.

401 Regarding the DOM fraction, Group A kept the highest COD content in DOM (26-38%)  
402 after AD. This could suggest that, DOM fraction could contain non-biodegradable  
403 compounds or that AD could produce accessible but complex molecules (Jimenez et al.,  
404 2015; Lashermes et al., 2009), which has also been shown during composting (Peltre et  
405 al., 2011). Indeed, Zhang et al. (2019) showed that refractory organic compounds (i.e.  
406 complex compounds) could be accumulated in DOM due to solubilization. In the  
407 studied dataset, the DOM fraction has been displayed to be variable among the groups.  
408 Actually, SPOM and DOM digestates spectra have been observed to present  
409 differences, although without a significative general trend (see Supplementary  
410 Material).

411 The SEOM fraction was kept similar or increased depending on the group. Laera et al.  
412 (2019) have also noticed a SEOM fraction increase from 7 to 15% after AD. These  
413 authors have associated it with the concentration of protein from the growth/decay of  
414 microorganisms and to a preferable consumption of simple soluble compounds.  
415 Similarly, the SEOM reduction was smaller compared with SPOM and REOM fractions  
416 for sewage sludge and cow manure digestion, as they are expected to have more  
417 complex and therefore less degradable compounds (Somers et al., 2021; Zhang et al.,  
418 2019). The FCI of SEOM has tended to increase in the digestate of Groups A and C.  
419 Meanwhile, the FCI of SEOM of Group B and D remained constant, whilst the SEOM  
420 accessibility decreased, probably due to the biodegradation of non-fluorescent  
421 compounds, as previously reported by Aemig et al. (2019).

422 PEOM fraction has also varied among feedstock types. The Groups with high initial  
423 PEOM fraction (B and C) has shown a decrease while an increase was observed for the  
424 Groups with low initial PEOM fraction (A and D). Similar findings were previously  
425 reported in Bareha et al. (2018) and Aemig et al. (2016). These authors have reported a  
426 PEOM fraction decrease for cow manure (i.e. rich in PEOM) and an increase for sewage  
427 sludge (i.e. poor in PEOM), respectively. Therefore, higher degradation rates of PEOM  
428 fraction (cellulose and hemicellulose) during AD could be expected when other simpler  
429 molecules are missing (Tambone et al., 2013). Biodegradable cellulose/hemicellulose in  
430 the PEOM fraction of Groups B and C have probably contributed to higher  
431 biodegradability of the PEOM fraction. However, the PEOM fraction of Groups A and  
432 D could contain non-identified complex compounds (e.g. complex proteins) that  
433 increase the recalcitrance to AD. The FCI of PEOM has increased for all groups (except  
434 for Group C). In contrast, Aemig et al. (2016) have reported no evolution on the FCI for  
435 the less accessible fractions during sewage sludge digestion. Nevertheless, a slight  
436 increase of the fluorescence intensity of humic-like compounds peaks in PEOM fraction  
437 after AD (suggesting poor biodegradability and high complexity of this fraction), was  
438 reported as a possible re-polymerization of humic acid (Tang et al., 2018; Zhang et al.,  
439 2019).

440 The NEOM fraction has increased for all groups after AD and represented between 25  
441 and 63% of the total COD in digestates. This lignocellulose-type fraction is  
442 concentrated after AD due to its recalcitrance and poor biodegradability in anaerobic  
443 conditions (Usman Khan and Kiaer Ahring, 2021). Thus, digestates are expected to be  
444 enriched in recalcitrant compounds, enhancing their suitability as soil amendment  
445 compared to the raw substrates (Jimenez et al., 2017; Pognani et al., 2010; Shakeri  
446 Yekta et al., 2019; Teglia et al., 2011b).

447 The obtained results have shown that the OM conversions shared a similar pattern  
448 regardless of the feedstock type: (i) an increase of complexity for the majority of the  
449 fractions, (ii) a global decrease of accessibility of the most accessible fractions (SPOM  
450 and REOM), and (iii) an increase of the non-extractable organic matter (NEOM)  
451 fraction. Nonetheless, it should be noted that the discussed evolution of the OM quality  
452 does not distinguish between the contribution due to the exogenous OM (i.e. substrate)  
453 and the endogenous OM (i.e. microbial-related products). The contribution of each  
454 compartment will be prioritized in forthcoming studies.

455 The accessibility conversion pattern is in agreement with Aemig et al. (2016), who have  
456 also shown a decrease for the most accessible fractions (named DOM, S-EPS and RE-  
457 EPS) during AD (22-65%, 49-50%, 23-35%, respectively), whereas NEOM relatively  
458 increased. Similarly, cow manure AD was evaluated by Somers et al. (2021) and a  
459 significant decrease in DOM, SPOM and REOM fractions of 24%, 62%, and 61%, was  
460 associated with methane production and hydrolysis of organic matter. Laera et al.  
461 (2019) have also noted a remarkable decrease from 76 to 28% for the DOM fraction  
462 between raw and digested mixtures of household, slaughterhouse and industrial wastes.  
463 Besides, an increase from 9% to 47% for PEOM + NEOM was also reported by these  
464 authors. Moreover, Zhang et al. (2019) have also showed a decrease after AD from  
465 46.74% to 39.42% for DOM, SPOM and REOM fractions and the FCI increased for all  
466 the extracted fractions. Furthermore, the FCI of the REOM fraction was increased by  
467 34% during cow manure AD (Somers et al., 2021) whereas a non-significant increase in  
468 the FCI of SEOM and PEOM during sludge and cow manure AD was stated by Aemig  
469 et al. (2019, 2016) and Somers et al. (2021), respectively. Therefore, general trends on  
470 OM accessibility and complexity evolution during AD have been observed.

471 Additionally, the prediction of OM accessibility and complexity of digestates from their  
472 inputs have been further assessed.

473

### 474 **3.3. Prediction of digestate OM quality from substrate OM quality**

#### 475 ***3.3.1. PLS model for the prediction of digestate OM quality***

476 PLS regression was applied on 28 observations (substrate/digestate pair) split in two  
477 datasets: a calibration dataset (23 samples) and a validation dataset (5 samples). Seven  
478 models were tested (Table 4). Model n°1 used the substrate fractions DOM+SPOM,  
479 REOM, SEOM and PEOM as X-variables to predict the digestate fractions (i.e.  
480 DOM+SPOM, REOM, SEOM and PEOM). NEOM fraction was not included as this  
481 fraction is calculated by difference. Model n°2 was similar to Model n°1 with the  
482 addition of the reactor temperature (T) as X-Variable. Model n°3 was the Model n°1  
483 with the addition of Hydraulic Retention Time (HRT) as X-Variables and Model n°4  
484 merged Models n°2 and 3.

485 Model n°5 used both fractions and fluorescence percentage in each fraction measured in  
486 the substrates (32 variables) as X-variables to predict the same 32 Y-variables in the  
487 digestates. Models n°6, 7 and 8 were based on Model n°5 with the addition of the T,  
488 HRT and both variables as X-variables, respectively. Table 4 presents the quality  
489 parameters of each model. The errors of calibration, cross-validation and prediction  
490 using cross-validation methods (RMSE, RMSE\_CV, and RSMEP) of each Y-variable in  
491 each model are specified in the Supplementary Material.

492 According to Table 4, all the models have shown good quality performances with  $Q^2 >$   
493 0.5 and correlation coefficients of prediction were between 0.691 and 0.832. Models n°5  
494 to 8 had better correlation coefficients than Models n°1 to 4 and smaller calibration

495 errors (cf. RMSE in Supplementary Material). Indeed, the addition of fluorescence  
496 variables from Model n°1 to n°5 improved the prediction of the 32 variables with 7  
497 components. Overall, for Model n°5,  $R^2$  was 0.831 and specific  $R^2$  for each fraction  
498 prediction was 0.869, 0.910, 0.736 and 0.882 for respectively DOM+SPOM, REOM,  
499 SEOM and PEOM. Furthermore, the prediction error RMSEP was lower in Model n°5  
500 for the fractions prediction than Model n°1 (see Supplementary Material).

501 The Model n°2 and 4 had the best performances among the models using only fractions  
502 and operational parameters as X-Variables. Indeed, the addition of T (Model n°2) and  
503 the addition of HRT (Model n°3) as X-variables increased  $R^2Y$  but needed a component  
504 addition. However, HRT addition did not improve the quality parameters  $R^2Y$  and  $Q^2$   
505 (Model n°4 in Table 4). This trend was not the same in the case of Models n°6 to 8 in  
506 comparison with Model n°5 without operational parameters. Indeed, despite a little  
507 increase of  $R^2Y$  when T was added as X-variables (Model N°6), the prediction accuracy  
508 ( $Q^2$ ) was decreased when HRT and T were added. The results obtained in Model n°2  
509 have shown that T was anti-correlated (p-value < 0.05) with SEOM ( $R^2 = -0.593$ ) and,  
510 less significantly with DOM+SPOM ( $R^2 = -0.313$ ). However, reactors T were mainly  
511 mesophilic except for MW digestates (55 °C). These digestates were associated with  
512 lower DOM+SPOM and SEOM fractions than the others. Consequently, relying on our  
513 dataset, the impact of T was related to the substrate type. To test the impact of T alone,  
514 it would have been interesting to get substrate/digestate pairs from various feedstocks at  
515 both mesophilic and thermophilic temperature.

516 Similarly, the obtained results in Model n°3 have shown that HRT was negatively  
517 correlated with REOM ( $R^2 = -0.628$ ) and, positively correlated with PEOM ( $R^2 =$   
518 0.397). However, low HRT values were mainly found for sludge digestion whereas  
519 high HRT values were associated with cow manure digestates. Sludge digestate groups

520 were related to a high value of REOM and SEOM fractions whereas cow manure  
521 digestates were characterized by high values of PEOM and low values of DOM+SPOM.  
522 Again, it was not possible to distinguish the effect of HRT from substrate impact on  
523 digestate quality prediction. Moreover, in the Model n°4, weight coefficients showed  
524 that HRT and T were considered as the least important variables for quality prediction  
525 (Supplementary Material).

526 As the operational conditions have been determined as non-explicative enough in this  
527 study, and considering the high quality of the prediction, Model n°5 was selected.

528 Besides, the predicted variables of digestates quality are necessary for the PLS model  
529 for C biodegradability in soil. To go further, the impact of the most significant X-  
530 variables affecting the prediction of Y-variables derived from the calculation of the  
531 weight of each variable for Model n°5 (without T and HRT) was analyzed (data not  
532 shown).

533 The characteristics of input OM remarkably influenced the prediction of the digestate  
534 OM characteristics, meaning that the main pattern of accessibility present in feedstock  
535 input remained in digestate OM after AD. The variables of the most complex  
536 fluorescence zones from substrate impacted significantly the digestate quality. The  
537 recalcitrant compounds contained in the substrate were preserved in their subsequent  
538 digestate, as possible humus precursors (Guilayn et al., 2020; Tambone et al., 2010).  
539 Nonetheless, for the prediction of the simpler fluorescence zones, other factors such as:  
540 (i) solubilisation/complexification of biodegradable/non-biodegradable compounds, (ii)  
541 preferential compounds degradation, (iii) hydrolysis, (iv) prevalence of recalcitrant  
542 compounds, (iv) compounds contribution from other fractions are possible hypothesis  
543 that contribute to the explanation of the resulting prediction. Therefore, this is the first  
544 approach to understand how OM quality varies with AD based on accessibility and

545 complexity for a wide range of feedstock. The addition of the T and the HRT as X-  
546 variables to predict OM quality and accessibility confirmed that the operational  
547 conditions were not informative enough for the studied dataset. To properly evaluate the  
548 impact of the operational conditions on the prediction of digestate quality, the digestion  
549 of the same substrate subjected to different T or HRT should be conceived in future  
550 investigations.

### 551 ***3.3.2. Coupling digestate quality prediction with PLS model for carbon*** 552 ***biodegradability in soil prediction***

553 To validate the digestate quality PLS model found, the PLS model for C  
554 biodegradability in soil was applied on the digestate quality predicted by Model n°5.  
555 Among all the samples that were used for the digestate quality model, 14 samples were  
556 incubated in soil and biodegradable carbon (C\_bio) was obtained after 91 days (Table  
557 2).

558 First, the PLS model for C biodegradability in soil was tested. A comparison between  
559 the 14 predicted values of proportion of biodegradable C in the digestates and  
560 experimental data obtained through soil incubation was plotted in Figure 4a. Results  
561 have shown that the PLS model for C biodegradability in soil was successfully able to  
562 predict the biodegradable organic C of the 14 digestates ( $R^2 = 0.739$ ) with low bias.  
563 Then, Model n°5 was combined with the PLS model for C biodegradability in soil to  
564 predict C\_bio. Figure 4b shows that the C\_bio prediction was not altered by the models'  
565 combination. Indeed, the combined models were able to predict the experimental data  
566 ( $R^2 = 0.697$ ) with a similar bias as in Jimenez et al. (2017). The 5 validation samples  
567 that were used for Model n°5 were plotted in black in Figure 4a and b. Prediction error  
568 of C\_bio obtained by the combined models ranged between 1% and 7%, with  $R^2 =$



569 0.828, which represents a high quality of prediction. Therefore, the reproducibility of  
570 the model was confirmed. Moreover, the model validation was performed with external  
571 data not included in the dataset used for model calibration. Finally, the 28 pair samples  
572 were used to compare both models' predictions as presented in Figure 4c. Results  
573 showed that C\_bio prediction by the combined models is quite similar to C\_bio  
574 prediction by Jimenez et al. (2017) ( $R^2 = 0.894$ ).

575 Thus, Model n°5 provided an extra step on OM fate prediction from raw substrate to soil  
576 C mineralization to better understand AD influence on OM accessibility and complexity  
577 before land disposal. Additionally, the present study related multiple aspects of  
578 scientific interest such as waste characterization, anaerobic transformation processes of  
579 OM and soil C mineralization and supposes an innovative approach to enhance the  
580 modeling of the AD process chain. Nonetheless, future actions could be addressed to  
581 improve the models' application when specific substrates are subjected to different AD  
582 operational conditions and soil typologies.

583

#### 584 **4. Conclusions**

585 The prediction of digestate OM quality from their input was evaluated. PCA and HCA  
586 analysis have allowed to classify 28 substrate/digestate pairs covering a wide diversity  
587 of OM. This classification was based on the extracted fractions from the OM  
588 (accessibility) and their complexity assessed by fluorescence. Substrates and their  
589 respective digestates were clustered together according to the feedstock type.  
590 Nonetheless, common trends on the conversions of OM quality were observed,  
591 indicating potential for the prediction of digestate quality of the entire dataset regardless  
592 of the feedstock type. Thus, this study proposed a digestate quality PLS model that

593 accurately predicted ( $Q^2 = 0.593$ ) the digestates OM quality from the substrate OM  
594 characteristics. However, future investigations should be focused on subjecting the same  
595 substrate to different T or HRT to properly evaluate the impact of operational conditions  
596 on the prediction of digestate quality. The predicted digestate OM characteristics  
597 validated the prediction of their biodegradability in soils using the PLS model for C  
598 biodegradability in soil previously developed. This work performed the combination of  
599 both models. OM conversion during AD and soil C mineralization was precisely  
600 predicted using a rapid analysis indicator (biochemical fractionation and 3D  
601 fluorescence). Such combined models brought a major contribution in the modeling of  
602 the AD process chain favoring the development of decision-making tools to properly  
603 manage the digestates.

604

## 605 **Acknowledgements**

606 This research was financially supported by the French Occitanie Region (No.  
607 00004786-24001447) and the French National Research Institute for Agriculture, Food  
608 and Environment (INRAE). The authors are thankful for some of the data retrieved from  
609 the DIGESTATE project, funded by ANR (Agence Nationale de la Recherche, France)  
610 under the Grant ANR-15- CE34-0003-01. The authors also wish to thank Lucía Braga  
611 for her useful remarks.

612

## 613 **References**

614 Aemig, Q., Chéron, C., Delgenès, N., Jimenez, J., Houot, S., Steyer, J.-P., Patureau, D., 2016.  
615 Distribution of Polycyclic Aromatic Hydrocarbons (PAHs) in sludge organic matter  
616 pools as a driving force of their fate during anaerobic digestion. *Waste Manag.* 48, 389–  
617 396. <https://doi.org/10.1016/j.wasman.2015.11.045>

618 Aemig, Q., Doussiet, N., Danel, A., Delgenès, N., Jimenez, J., Houot, S., Patureau, D., 2019.  
619 Organic micropollutants' distribution within sludge organic matter fractions explains  
620 their dynamic during sewage sludge anaerobic digestion followed by composting.  
621 *Environ. Sci. Pollut. Res.* 26, 5820–5830. <https://doi.org/10.1007/s11356-018-4014-7>  
622 Akhiar, A., Battimelli, A., Torrijos, M., Carrere, H., 2017. Comprehensive characterization of  
623 the liquid fraction of digestates from full-scale anaerobic co-digestion. *Waste Manag.*  
624 59, 118–128. <https://doi.org/10.1016/j.wasman.2016.11.005>  
625 Akhiar, A., Guilayn, F., Torrijos, M., Battimelli, A., Shamsuddin, A.H., Carrère, H., 2021.  
626 Correlations between the Composition of Liquid Fraction of Full-Scale Digestates and  
627 Process Conditions. *Energies* 14, 971. <https://doi.org/10.3390/en14040971>  
628 APHA, 2005. *Standard Methods for the Examination of Water and Waste-Water*, 22nd ed.  
629 Washington, DC.  
630 Bareha, Y., Girault, R., Guezel, S., Chaker, J., Trémier, A., 2019. Modeling the fate of organic  
631 nitrogen during anaerobic digestion: Development of a bioaccessibility based ADM1.  
632 *Water Res.* 154, 298–315. <https://doi.org/10.1016/j.watres.2019.02.011>  
633 Bareha, Y., Girault, R., Jimenez, J., Trémier, A., 2018. Characterization and prediction of  
634 organic nitrogen biodegradability during anaerobic digestion: A bioaccessibility  
635 approach. *Bioresour. Technol.* 263, 425–436.  
636 <https://doi.org/10.1016/j.biortech.2018.04.085>  
637 Fang, F., Hu, H.-L., Qin, M.-M., Xue, Z.-X., Cao, J.-S., Hu, Z.-R., 2015. Effects of metabolic  
638 uncouplers on excess sludge reduction and microbial products of activated sludge.  
639 *Bioresour. Technol.* 185, 1–6. <https://doi.org/10.1016/j.biortech.2015.02.054>  
640 Fernandes, T.V., Klaasse Bos, G.J., Zeeman, G., Sanders, J.P.M., van Lier, J.B., 2009. Effects  
641 of thermo-chemical pre-treatment on anaerobic biodegradability and hydrolysis of  
642 lignocellulosic biomass. *Bioresour. Technol.* 100, 2575–2579.  
643 <https://doi.org/10.1016/j.biortech.2008.12.012>  
644 Fernandez-Bayo, J.D., Yazdani, R., Simmons, C.W., VanderGheynst, J.S., 2018. Comparison of  
645 thermophilic anaerobic and aerobic treatment processes for stabilization of green and  
646 food wastes and production of soil amendments. *Waste Manag.* 77, 555–564.  
647 <https://doi.org/10.1016/j.wasman.2018.05.006>  
648 Fernández-Domínguez, D., Astals, S., Peces, M., Frison, N., Bolzonella, D., Mata-Alvarez, J.,  
649 Dosta, J., 2020. Volatile fatty acids production from biowaste at mechanical-biological  
650 treatment plants: Focusing on fermentation temperature. *Bioresour. Technol.* 314,  
651 123729. <https://doi.org/10.1016/j.biortech.2020.123729>  
652 Fonoll, X., Astals, S., Dosta, J., Mata-Alvarez, J., 2016. Impact of paper and cardboard  
653 suppression on OFMSW anaerobic digestion. *Waste Manag.* 56, 100–105.  
654 <https://doi.org/10.1016/j.wasman.2016.05.023>  
655 Guilayn, F., Jimenez, J., Martel, J.-L., Rouez, M., Crest, M., Patureau, D., 2019. First  
656 fertilizing-value typology of digestates: A decision-making tool for regulation. *Waste*  
657 *Manag.* 86, 67–79. <https://doi.org/10.1016/j.wasman.2019.01.032>  
658 Guilayn, F., Rouez, M., Crest, M., Patureau, D., Jimenez, J., 2020. Valorization of digestates  
659 from urban or centralized biogas plants: a critical review. *Rev. Environ. Sci.*  
660 *Biotechnol.* 19. <https://doi.org/10.1007/s11157-020-09531-3>  
661 Gunaseelan, V.N., 2007. Regression models of ultimate methane yields of fruits and vegetable  
662 solid wastes, sorghum and napiergrass on chemical composition. *Bioresour. Technol.*  
663 98, 1270–1277. <https://doi.org/10.1016/j.biortech.2006.05.014>  
664 Guo, X., Li, C., Zhu, Q., Huang, T., Cai, Y., Li, N., Liu, J., Tan, X., 2018. Characterization of  
665 dissolved organic matter from biogas residue composting using spectroscopic  
666 techniques. *Waste Manag.* 78, 301–309. <https://doi.org/10.1016/j.wasman.2018.06.001>  
667 He, X.-S., Xi, B.-D., Wei, Z.-M., Jiang, Y.-H., Yang, Y., An, D., Cao, J.-L., Liu, H.-L., 2011.  
668 Fluorescence excitation–emission matrix spectroscopy with regional integration  
669 analysis for characterizing composition and transformation of dissolved organic matter  
670 in landfill leachates. *J. Hazard. Mater.* 190, 293–299.  
671 <https://doi.org/10.1016/j.jhazmat.2011.03.047>

- 672 Insam, H., Gómez-Brandón, M., Ascher, J., 2015. Manure-based biogas fermentation residues –  
673 Friend or foe of soil fertility? *Soil Biol. Biochem.* 84, 1–14.  
674 <https://doi.org/10.1016/j.soilbio.2015.02.006>
- 675 Jimenez, J., Gonidec, E., Cacho Rivero, J.A., Latrille, E., Vedrenne, F., Steyer, J.-P., 2014.  
676 Prediction of anaerobic biodegradability and bioaccessibility of municipal sludge by  
677 coupling sequential extractions with fluorescence spectroscopy: Towards ADM1  
678 variables characterization. *Water Res.* 50, 359–372.  
679 <https://doi.org/10.1016/j.watres.2013.10.048>
- 680 Jimenez, J., Aemig, Q., Doussiet, N., Steyer, J.-P., Houot, S., Patureau, D., 2015. A new organic  
681 matter fractionation methodology for organic wastes: Bioaccessibility and complexity  
682 characterization for treatment optimization. *Bioresour. Technol.* 194, 344–353.  
683 <https://doi.org/10.1016/j.biortech.2015.07.037>
- 684 Jimenez, J., Lei, H., Steyer, J.-P., Houot, S., Patureau, D., 2017. Methane production and  
685 fertilizing value of organic waste: Organic matter characterization for a better prediction  
686 of valorization pathways. *Bioresour. Technol.* 241, 1012–1021.  
687 <https://doi.org/10.1016/j.biortech.2017.05.176>
- 688 Jimenez, J., Charnier, C., Kouas, M., Latrille, E., Torrijos, M., Harmand, J., Patureau, D.,  
689 Spérandio, M., Morgenroth, E., Béline, F., Ekama, G., Vanrolleghem, P.A., Robles, A.,  
690 Seco, A., Batstone, D.J., Steyer, J.-P., 2020. Modelling hydrolysis: Simultaneous versus  
691 sequential biodegradation of the hydrolysable fractions. *Waste Manag.* 101, 150–160.  
692 <https://doi.org/10.1016/j.wasman.2019.10.004>
- 693 Khakbaz, A., Nobili, M.D., Mainardis, M., Contin, M., Aneggi, E., Mattiussi, M., Cabras, I.,  
694 Busut, M., Goi, D., 2020. Monitoring of heavy metals, eox and las in sewage sludge for  
695 agricultural use: a case study. *Detritus* 160. [https://doi.org/10.31025/2611-](https://doi.org/10.31025/2611-4135/2020.13993)  
696 [4135/2020.13993](https://doi.org/10.31025/2611-4135/2020.13993)
- 697 Kögel-Knabner, I., 2002. The macromolecular organic composition of plant and microbial  
698 residues as inputs to soil organic matter. *Soil Biol. Biochem.* 34, 139–162.  
699 [https://doi.org/10.1016/S0038-0717\(01\)00158-4](https://doi.org/10.1016/S0038-0717(01)00158-4)
- 700 Laera, A., Shakeri Yekta, S., Hedenström, M., Buzier, R., Guibaud, G., Dario, M., Esposito, G.,  
701 van Hullebusch, E.D., 2019. A simultaneous assessment of organic matter and trace  
702 elements bio-accessibility in substrate and digestate from an anaerobic digestion plant.  
703 *Bioresour. Technol.* 288, 121587. <https://doi.org/10.1016/j.biortech.2019.121587>
- 704 Lashermes, G., Nicolardot, B., Parnaudeau, V., Thuriès, L., Chaussod, R., Guillotin, M.L.,  
705 Linères, M., Mary, B., Metzger, L., Morvan, T., Tricaud, A., Villette, C., Houot, S.,  
706 2009. Indicator of potential residual carbon in soils after exogenous organic matter  
707 application. *Eur. J. Soil Sci.* 60, 297–310. [https://doi.org/10.1111/j.1365-](https://doi.org/10.1111/j.1365-2389.2008.01110.x)  
708 [2389.2008.01110.x](https://doi.org/10.1111/j.1365-2389.2008.01110.x)
- 709 Levavasseur, F., Mary, B., Houot, S., 2021. C and N dynamics with repeated organic  
710 amendments can be simulated with the STICS model. *Nutr. Cycl. Agroecosystems* 119,  
711 103–121. <https://doi.org/10.1007/s10705-020-10106-5>
- 712 Maynaud, G., Druilhe, C., Daumoin, M., Jimenez, J., Patureau, D., Torrijos, M., Pourcher, A.-  
713 M., Wéry, N., 2017. Characterisation of the biodegradability of post-treated digestates  
714 via the chemical accessibility and complexity of organic matter. *Bioresour. Technol.*  
715 231, 65–74. <https://doi.org/10.1016/j.biortech.2017.01.057>
- 716 Minasny, B., Malone, B.P., McBratney, A.B., Angers, D.A., Arrouays, D., Chambers, A.,  
717 Chaplot, V., Chen, Z.-S., Cheng, K., Das, B.S., Field, D.J., Gimona, A., Hedley, C.B.,  
718 Hong, S.Y., Mandal, B., Marchant, B.P., Martin, M., McConkey, B.G., Mulder, V.L.,  
719 O'Rourke, S., Richer-de-Forges, A.C., Odeh, I., Padarian, J., Paustian, K., Pan, G.,  
720 Poggio, L., Savin, I., Stolbovoy, V., Stockmann, U., Sulaeman, Y., Tsui, C.-C., Vågen,  
721 T.-G., van Wesemael, B., Winowiecki, L., 2017. Soil carbon 4 per mille. *Geoderma*  
722 292, 59–86. <https://doi.org/10.1016/j.geoderma.2017.01.002>
- 723 Mottet, A., François, E., Latrille, E., Steyer, J.P., Déléris, S., Vedrenne, F., Carrère, H., 2010.  
724 Estimating anaerobic biodegradability indicators for waste activated sludge. *Chem. Eng.*  
725 *J.* 160, 488–496. <https://doi.org/10.1016/j.cej.2010.03.059>

726 Mottet, A., Ramirez, I., Carrère, H., Déléris, S., Vedrenne, F., Jimenez, J., Steyer, J.P., 2013.  
727 New fractionation for a better bioaccessibility description of particulate organic matter  
728 in a modified ADM1 model. *Chem. Eng. J.* 228, 871–881.  
729 <https://doi.org/10.1016/j.cej.2013.05.082>

730 Muller, M., Jimenez, J., Antonini, M., Dudal, Y., Latrille, E., Vedrenne, F., Steyer, J.-P.,  
731 Patureau, D., 2014. Combining chemical sequential extractions with 3D fluorescence  
732 spectroscopy to characterize sludge organic matter. *Waste Manag.* 34, 2572–2580.  
733 <https://doi.org/10.1016/j.wasman.2014.07.028>

734 Peltre, C., Thuriès, L., Barthès, B., Brunet, D., Morvan, T., Nicolardot, B., Parnaudeau, V.,  
735 Houot, S., 2011. Near infrared reflectance spectroscopy: A tool to characterize the  
736 composition of different types of exogenous organic matter and their behaviour in soil.  
737 *Soil Biol. Biochem.* 43, 197–205. <https://doi.org/10.1016/j.soilbio.2010.09.036>

738 Pognani, M., Barrera, R., Font, X., Scaglia, B., Adani, F., Sánchez, A., 2010. Monitoring the  
739 organic matter properties in a combined anaerobic/aerobic full-scale municipal source-  
740 separated waste treatment plant. *Bioresour. Technol.* 101, 6873–6877.  
741 <https://doi.org/10.1016/j.biortech.2010.03.110>

742 Provenzano, M.R., Iannuzzi, G., Fabbri, C., Senesi, N., 2011. Qualitative Characterization and  
743 Differentiation of Digestates from Different Biowastes Using FTIR and Fluorescence  
744 Spectroscopies. *J. Environ. Prot.* 2, 83–89. <https://doi.org/10.4236/jep.2011.21009>

745 Provenzano, M.R., Malerba, A.D., Pezzolla, D., Gigliotti, G., 2014. Chemical and spectroscopic  
746 characterization of organic matter during the anaerobic digestion and successive  
747 composting of pig slurry. *Waste Manag.* 34, 653–660.  
748 <https://doi.org/10.1016/j.wasman.2013.12.001>

749 Rocamora, I., Wagland, S.T., Villa, R., Simpson, E.W., Fernández, O., Bajón-Fernández, Y.,  
750 2020. Dry anaerobic digestion of organic waste: A review of operational parameters and  
751 their impact on process performance. *Bioresour. Technol.* 299, 122681.  
752 <https://doi.org/10.1016/j.biortech.2019.122681>

753 Shakeri Yekta, S., Hedenström, M., Svensson, B.H., Sundgren, I., Dario, M., Enrich-Prast, A.,  
754 Hertkorn, N., Björn, A., 2019. Molecular characterization of particulate organic matter  
755 in full scale anaerobic digesters: An NMR spectroscopy study. *Sci. Total Environ.* 685,  
756 1107–1115. <https://doi.org/10.1016/j.scitotenv.2019.06.264>

757 Soest, V., J, P., 1963. Use of detergents in the analysis of fibrous feeds. 2. A rapid method for  
758 the determination of fiber and lignin. *J. Assoc. Off. Agric. Chem.* 46, 829–835.

759 Somers, M.H., Jimenez, J., Azman, S., Steyer, J.-P., Baeyens, J., Appels, L., 2021.  
760 Ultrasonication affects the bio-accessibility of primary dairy cow manure digestate for  
761 secondary post-digestion. *Fuel* 291, 120140. <https://doi.org/10.1016/j.fuel.2021.120140>

762 Tambone, F., Adani, F., Gigliotti, G., Volpe, D., Fabbri, C., Provenzano, M.R., 2013. Organic  
763 matter characterization during the anaerobic digestion of different biomasses by means  
764 of CPMAS <sup>13</sup>C NMR spectroscopy. *Biomass Bioenergy* 48, 111–120.  
765 <https://doi.org/10.1016/j.biombioe.2012.11.006>

766 Tambone, F., Terruzzi, L., Scaglia, B., Adani, F., 2015. Composting of the solid fraction of  
767 digestate derived from pig slurry: Biological processes and compost properties. *Waste*  
768 *Manag.* 35, 55–61. <https://doi.org/10.1016/j.wasman.2014.10.014>

769 Tambone, F., Orzi, V., Zilio, M., Adani, F., 2019. Measuring the organic amendment properties  
770 of the liquid fraction of digestate. *Waste Manag.* 88, 21–27.  
771 <https://doi.org/10.1016/j.wasman.2019.03.024>

772 Tang, Y., Li, X., Dong, B., Huang, J., Wei, Y., Dai, X., Dai, L., 2018. Effect of aromatic  
773 repolymerization of humic acid-like fraction on digestate phytotoxicity reduction during  
774 high-solid anaerobic digestion for stabilization treatment of sewage sludge. *Water Res.*  
775 143, 436–444. <https://doi.org/10.1016/j.watres.2018.07.003>

776 Development Core Team, R., 2021. R: A Language and Environment for Statistical Computing.  
777 R Foundation for Statistical Computing, Vienna, Austria.

778 Teglia, C., Tremier, A., Martel, J.-L., 2011a. Characterization of Solid Digestates: Part 1,  
779 Review of Existing Indicators to Assess Solid Digestates Agricultural Use. *Waste*  
780 *Biomass Valorization* 2, 43–58. <https://doi.org/10.1007/s12649-010-9051-5>

781 Teglia, C., Tremier, A., Martel, J.-L., 2011b. Characterization of Solid Digestates: Part 2,  
782 Assessment of the Quality and Suitability for Composting of Six Digested Products.  
783 Waste Biomass Valorization 2, 113–126. <https://doi.org/10.1007/s12649-010-9059-x>  
784 Triolo, J.M., Pedersen, L., Qu, H., Sommer, S.G., 2012. Biochemical methane potential and  
785 anaerobic biodegradability of non-herbaceous and herbaceous phytomass in biogas  
786 production. *Bioresour. Technol.* 125, 226–232.  
787 <https://doi.org/10.1016/j.biortech.2012.08.079>  
788 Usman Khan, M., Kiaer Ahring, B., 2021. Improving the biogas yield of manure: Effect of  
789 pretreatment on anaerobic digestion of the recalcitrant fraction of manure. *Bioresour.*  
790 *Technol.* 321, 124427. <https://doi.org/10.1016/j.biortech.2020.124427>  
791 Vidal-Antich, C., Perez-Esteban, N., Astals, S., Peces, M., Mata-Alvarez, J., Dosta, J., 2021.  
792 Assessing the potential of waste activated sludge and food waste co-fermentation for  
793 carboxylic acids production. *Sci. Total Environ.* 757, 143763.  
794 <https://doi.org/10.1016/j.scitotenv.2020.143763>  
795 Vinardell, S., Astals, S., Koch, K., Mata-Alvarez, J., Dosta, J., 2021. Co-digestion of sewage  
796 sludge and food waste in a wastewater treatment plant based on mainstream anaerobic  
797 membrane bioreactor technology: A techno-economic evaluation. *Bioresour. Technol.*  
798 330, 124978. <https://doi.org/10.1016/j.biortech.2021.124978>  
799 Zhang, Y., Xu, S., Cui, M., Wong, J.W.C., 2019. Effects of different thermal pretreatments on  
800 the biodegradability and bioaccessibility of sewage sludge. *Waste Manag.* 94, 68–76.  
801 <https://doi.org/10.1016/j.wasman.2019.05.047>  
802  
803  
804  
805  
806  
807  
808  
809  
810  
811  
812  
813  
814  
815

816 **Table 1.** Summary of the raw substrate/digestate pairs type, origin and digester  
 817 operational conditions

Type of feedstock <sup>a</sup>	Digestate type <sup>b</sup>	Number of substrate/digestate pairs	Scale	Origin	T (°C)	HRT (d)
Cow manure	4	5	Industrial	Farms	35-41	56-75
Cow manure mixtures:		2				
CM + Straw		1	Industrial	Farms	35-37	56
50% CM/S + 23% HM/S + 27% Slu		1	Industrial	Farms	35-37	56
Straw	1	1	Lab scale	Farms	-	-
Biowaste	2	1	Industrial	Municipal solid waste plant	55	21
Biowaste mixtures:		1				
50% BW + 20% CS + 30% AIW	5	1	Industrial	Municipal solid waste plant	37	90
Municipal Waste	5	4	Industrial	Municipal solid waste plant	55	20-28
Pig Slurry	3	1	Industrial	Farms	38	60
Pig Slurry mixtures:		6				
45% PS + 40% PsluAI + 15% others	3	1	Lab scale	Farms	38	60
93% PS + 7% Cow Food	3	1	Lab scale	Farms	38	24
93% PS + 7% Horse Food	3	1	Lab scale	Farms	38	24
80% PS + 20% Maize Silage	1	1	Lab scale	Farms	38	25
62% PS + 38% CM	1	1	Lab scale	Farms	38	24
80% PS + 20% BW	3	1	Lab scale	Farms	38	21
Sludge	2	7	Industrial	Wastewater treatment plant	37	15-25

818 <sup>a</sup>Type of feedstock: AIW: agroindustrial waste; BW: biowaste; CM: cow manure; CS: cow slurry; HM: horse manure; PS: pig  
 819 slurry; PsluAI: primary sludge from agroindustry; S: slurry; Slu: Sludge. <sup>b</sup>Digestate type based on Guilayn et al. (2019): (1) Fibrous  
 820 feedstock (2) Sewage sludge, Biowaste, food agroindustrial residues (FAI) mono/co-digestion; (3) Organic fraction of municipal  
 821 solid waste (OFMSW), Food waste (FW), FAI, PS mono/co-digestion; (4) Manure/other co-digestion; (5) OFMSW and BW  
 822 mono/co-digestion; (6) Fibrous feedstock: Cattle manure, green waste, silage.

823

824

825

826

827

828

829

830

831

832

833

834

835

836

837

838

839 **Table 2.** Biodegradable carbon percentage after soil incubation of several studied  
 840 digestates coming from Jimenez et al. (2017) data

Digestate name	C_bio (%C)
Sludge2_D	39%
Sludge7_D	31%
CM3_D	15%
MW1_D	25%
MW3_D	32%
MW4_D	19%
MW5_D	27%
PS +BW_D	46%
PS + Cow Food_D	43%
PS + Cow Manure_D	24%
PS + Horse Food_D	35%
PS + Maize Silage_D	44%
BW_D	24%
PS + PrimSluAI_D	31%

841  
 842  
 843  
 844  
 845  
 846  
 847  
 848  
 849  
 850  
 851  
 852  
 853  
 854  
 855  
 856  
 857  
 858



859 **Table 3.** Proportions of COD for each extracted fraction and fluorescence complexity  
 860 index evolution after AD in the different groups. The results display the relative  
 861 percentage of the increase or decrease as expressed in Tambone et al. (2013).

Group	Accessibility (% in COD)						Fluorescence complexity index (-)			
	DOM	SPOM	REOM	SEOM	PEOM	NEOM	SPOM	REOM	SEOM	PEOM
A	--	--	--	+	++	++	++++	++	+	++
B	N.A.	--	-	-	-	++	++	++	0	+
C	++++	---	--	++	--	+	--	-	+++	-
D	--	--	--	-	+	++	++	++	0	+++

862 Relative conversion ranges: +: 0 to 25%; ++: 25 to 50%; +++: 50 to 75%; ++++: 75 to 100%; -: 0 to -25%; --: -25 to -50%; ---: -50  
 863 to -75%; ----: -75 to -100%. Relative percentage = (final value in the digestates - initial value in the substrates)/initial value in the  
 864 substrates) × 100. N.A. = no presence of DOM for Group B (solid digestates)

865

866

867

868

869

870

871

872

873

874

875

876

877

878

879

880

881

882

883

884

885

886

887 **Table 4.** Quality parameters of the PLS models

Model	Variables		Model quality			
	X	Y	Components number	R <sup>2</sup> X	R <sup>2</sup> Y	Q <sup>2</sup>
Model n°1	DOM+SPOM; REOM; SEOM; PEOM	DOM+SPOM; REOM; SEOM; PEOM	2	0.892	0.691	0.621
Model n°2	DOM+SPOM; REOM; SEOM; PEOM;T	DOM+SPOM; REOM; SEOM; PEOM	3	0.919	0.763	0.681
Model n°3	DOM+SPOM; REOM; SEOM; PEOM;HRT	DOM+SPOM; REOM; SEOM; PEOM	3	0.922	0.757	0.639
Model n°4	DOM+SPOM; REOM; SEOM; PEOM;HRT;T	DOM+SPOM; REOM; SEOM; PEOM	4	0.938	0.775	0.587
Model n°5	DOM+SPOM; REOM; SEOM; PEOM;Pf_i	DOM+SPOM; REOM; SEOM; PEOM;Pf_i	7	0.953	0.831	0.593
Model n°6	DOM+SPOM; REOM; SEOM; PEOM;Pf_i;T	DOM+SPOM; REOM; SEOM; PEOM;Pf_i	7	0.950	0.832	0.588
Model n°7	DOM+SPOM; REOM; SEOM; PEOM;Pf_i; HRT	DOM+SPOM; REOM; SEOM; PEOM;Pf_i	7	0.951	0.829	0.58
Model n°8	DOM+SPOM; REOM; SEOM; PEOM;Pf_i;T;HRT	DOM+SPOM; REOM; SEOM; PEOM;Pf_i	7	0.949	0.830	0.576

888

889

890

891

892

893

894

895

896

897

898

899

900

901

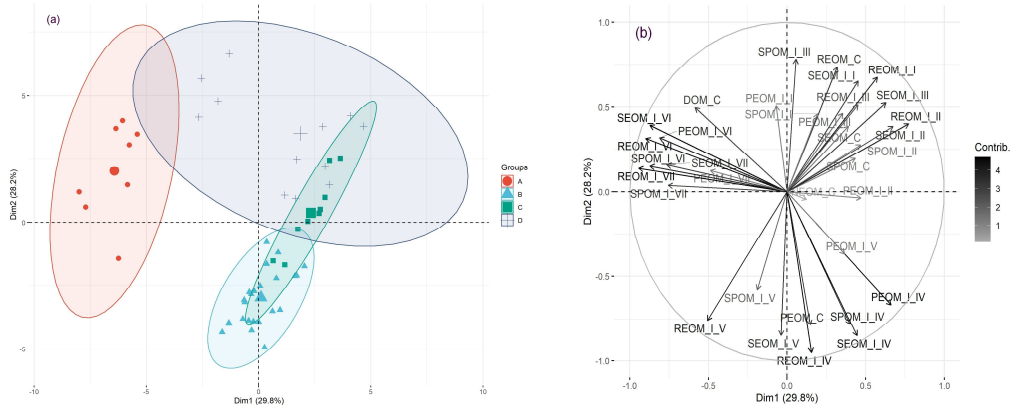
902

903

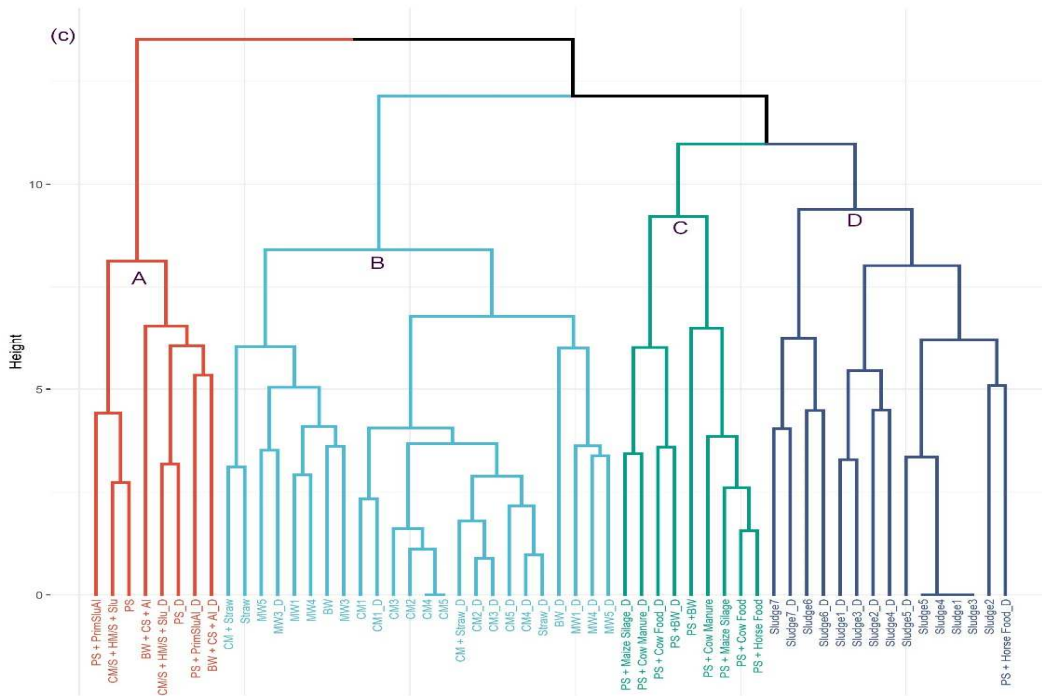
904

905

906



907



908

909 **Figure 1.** Scores plot (a) and loadings (b) obtained from the PCA analysis, and (c) HCA  
 910 analysis for the 56 samples studied. PCA individuals are distinguished by shape and  
 911 color according to the HCA revealed groups (A-D). Ellipses show 95% confidence  
 912 intervals. Loadings intensity color (plot b) is related to the variables contribution,  
 913 from low (1) to high (4). Groups: (A) pig slurry and slurry mixtures with primary  
 914 sludge, agro-industrial waste or biowaste, (B) manure, fibers and municipal solid waste,  
 915 (C) pig slurry mixtures with fiber or food wastes, and (D) sludge

916

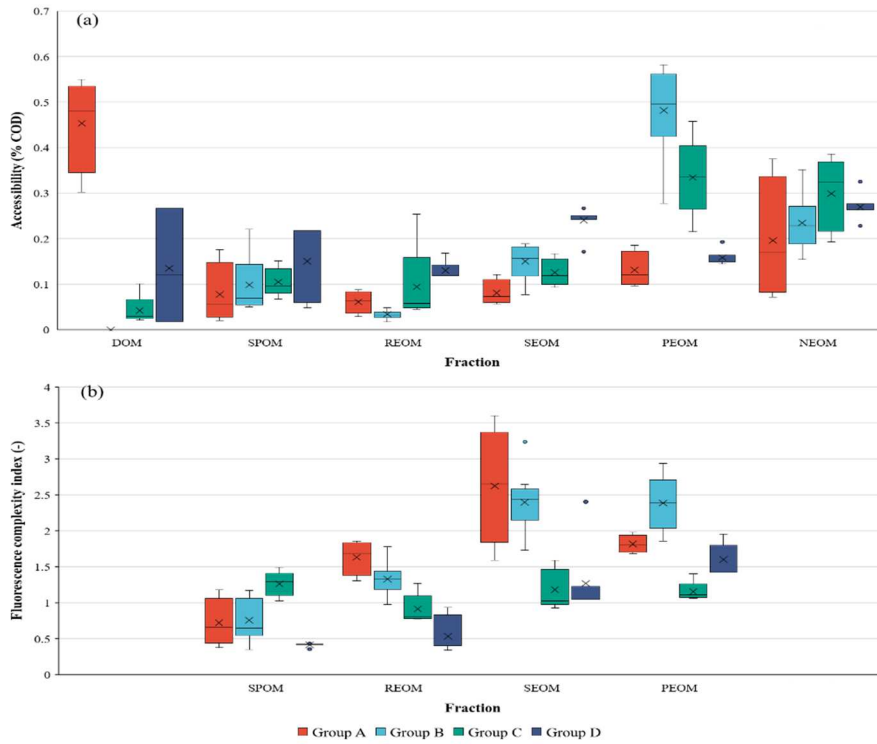
917

918

919

920

921



922

923  
924

925 **Figure 2.** Accessibility (a) and fluorescence complexity index (b) boxplots of substrates  
 926 for the HCA revealed groups. Groups: (A) pig slurry and slurry mixtures with primary  
 927 sludge, agro-industrial waste or biowaste, (B) manure, fibers and municipal solid waste,  
 928 (C) pig slurry mixtures with fiber or food wastes, and (D) sludge

929

930

931

932

933

934

935

936

937

938

939

940

941

942

943  
944  
945  
946  
947  
948  
949  
950  
951  
952  
953  
954  
955  
956  
957  
958  
959  
960  
961  
962  
963  
964  
965  
966  
967  
968  
969  
970

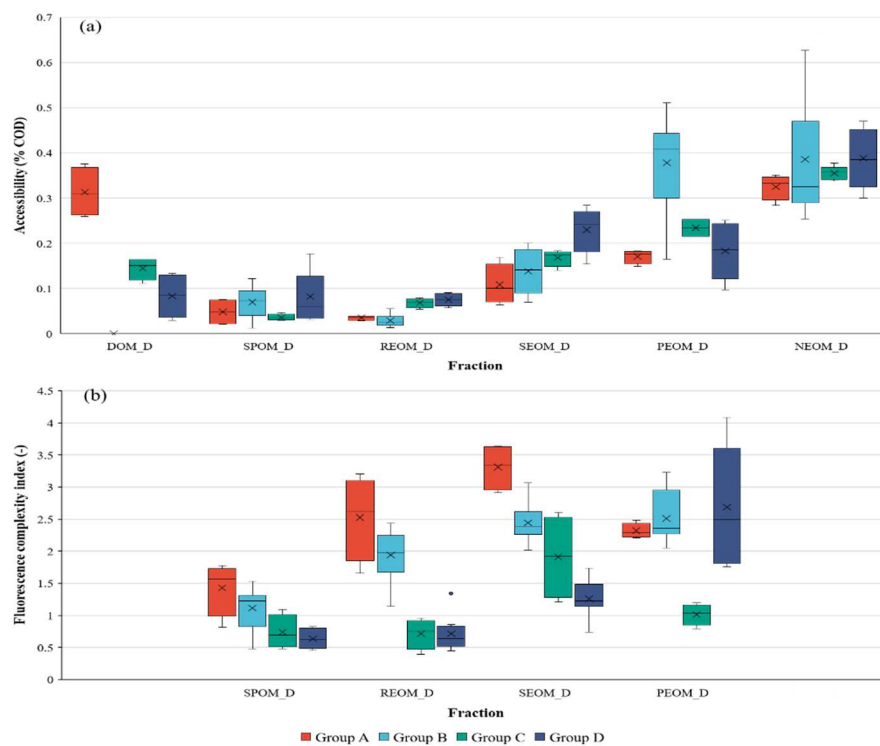
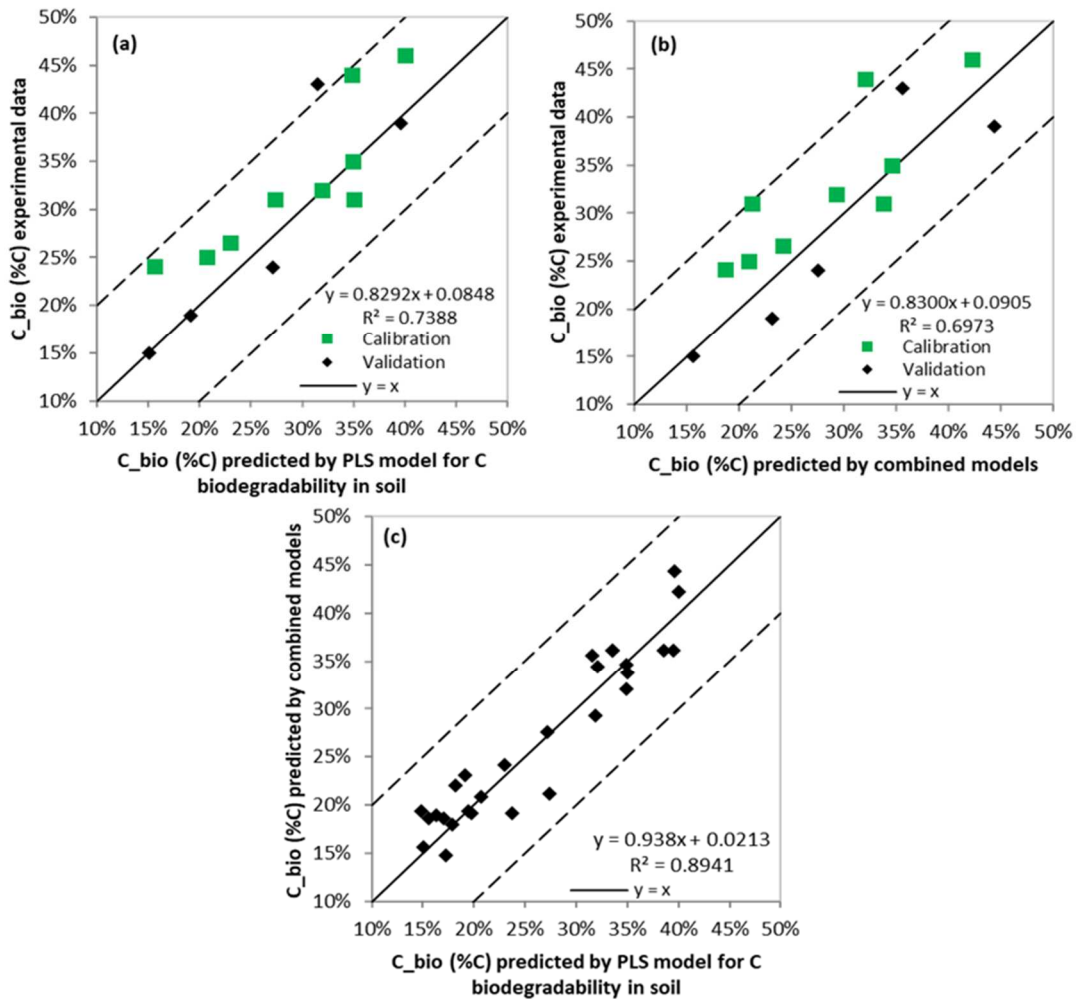


**Figure 3.** Accessibility (a) and fluorescence complexity index (b) boxplots of digestates for the HCA revealed groups. Groups: (A) pig slurry and slurry mixtures with primary sludge, agro-industrial waste or biowaste, (B) manure, fibers and municipal solid waste, (C) pig slurry mixtures with fiber or food wastes, and (D) sludge



971

972

973 **Figure 4.** Validation of model PLS: comparison between experimental data from  
 974 biodegradable organic carbon tests on soil with PLS model for C biodegradability in  
 975 soil (a) and combined models (b); and comparison between combined models and PLS  
 976 model for C biodegradability in soil (c)

977

978